Effects of dust contamination on the transverse dynamics of a magnetized electron plasma

M. Romé, F. Cavaliere, M. Cavenago, S. Chen, and G. Maero

Citation: AIP Conference Proceedings **1668**, 030001 (2015); doi: 10.1063/1.4923110

View online: http://dx.doi.org/10.1063/1.4923110

View Table of Contents: http://scitation.aip.org/content/aip/proceeding/aipcp/1668?ver=pdfcov

Published by the AIP Publishing

Effects of Dust Contamination on the Transverse Dynamics of a Magnetized Electron Plasma

M. Romé[*], F. Cavaliere[*], M. Cavenago[†], S. Chen[*,**] and G. Maero[*]

[*]*INFN Sezione di Milano and Dipartimento di Fisica, Università degli Studi di Milano, Via Celoria 16, I-20133 Milano, Italy*
[†]*INFN Laboratori Nazionali di Legnaro, Viale dell'Università 2, I-35020 Legnaro, Italy*
[**]*Institute of Fluid Physics, China Academy of Engineering Physics, Mianyang, China*

Abstract. Complex (dusty) plasmas are characterized by the presence of a fraction of micrometric or sub-micrometric particles which may collect a surface charge up to the order of a few thousand electron charges. The dusty plasmas studied in the experiments generally satisfy a global neutrality condition. By contrast, we present here the investigation of a magnetized nonneutral plasma, i.e., a plasma with a single sign of charge (e.g. electrons) confined in a Penning-Malmberg trap, contaminated by a dust population. We simulate the two-dimensional transverse dynamics of this multi-component plasma with a particle-in-cell code implementing a mass-less fluid (drift-Poisson) approximation for the electrons and a kinetic description for the dust component (including gravity). Simulations with different initial dust distributions and densities have been performed in order to investigate the influence of the dust on the development of the diocotron instability in the electron plasma. In particular, the early stage of the growth of the diocotron modes has been analyzed by Fourier decomposition.

Keywords: Nonneutral plasmas, dusty or complex plasmas, magnetized plasmas
PACS: 52.27.Jt, 52.27.Lw, 52.25.Xz

INTRODUCTION

A complex or dusty plasma is an ionized gas where particles with diameters in the range $0.01 - 10\ \mu$m are present in addition to electrons and ions. The dust grains acquire in the plasma a surface charge of the order of few hundreds or thousands electron charges. Due to their size, gravitational effects on the dust grains may be comparable to those arising from electric and magnetic fields. A peculiar feature of dusty plasmas is the interplay between a wide range of scales in space and time, and the occurrence of phenomena relevant to various fundamental aspects of plasma physics, hydrodynamics, and nonlinear physics [1]. The dusty plasmas studied in the laboratory are typically characterized by conditions of global quasi-neutrality and weak magnetization of the dust component. Only in a limited number of experiments, regimes of partial or complete magnetization of the dust populations have been investigated [2, 3].

On the other hand, magneto-electrostatic Penning-Malmberg traps are routinely used for the confinement of non-neutral plasmas, i.e. plasmas of particles with the same sign of charge, under ultra-high vacuum (UHV) conditions and strong magnetization of the trapped particles [4]. These conditions ensure very long storage times, allowing for a wide range of basic physics investigations [5, 6]. In particular, the dynamics of a trapped electron plasma is typically characterized by high values of the so-called 'rigidity parameter', i.e. the ratio between the frequency of the longitudinal bounce of the particles and that of the transverse drift. The electron dynamics is therefore essentially two-dimensional (2D), and exhibits a formal analogy with that of an ideal inviscid and incompressible fluid [7]. This provides the opportunity to investigate 2D fluid dynamical processes such as shear flow instabilities, vortex formation, and turbulence with experiments performed on trapped electron plasmas.

Here we investigate the dynamics of a nonneutral complex plasma, and more specifically of an electron plasma contaminated with a small fraction of charged dust particles of micro- and/or submicrometric size. This is the subject of the "DuEl" (Dust-Electron) project [8], which comprises the realization of a suitably modified Penning-Malmberg trap for the confinement of such a system. We describe here the present status of the apparatus. The project shows aspects of significant novelty in the field of complex plasmas, with a combination of plasma magnetization, nonneutrality and dust contamination. A particular goal is the analysis of the effects of dust on the instabilities and the evolution of the turbulence of the electron component [9]. The analysis is restricted so far to the transverse dynamics of the system.

Numerical investigations of the transverse dynamics of a dust-contaminated electron plasma have been performed by means of a recently developed 2D PIC code [10]. The code implements a mass-less fluid (drift-Poisson) approximation

Non-Neutral Plasma Physics IX
AIP Conf. Proc. 1668, 030001-1–030001-8; doi: 10.1063/1.4923110

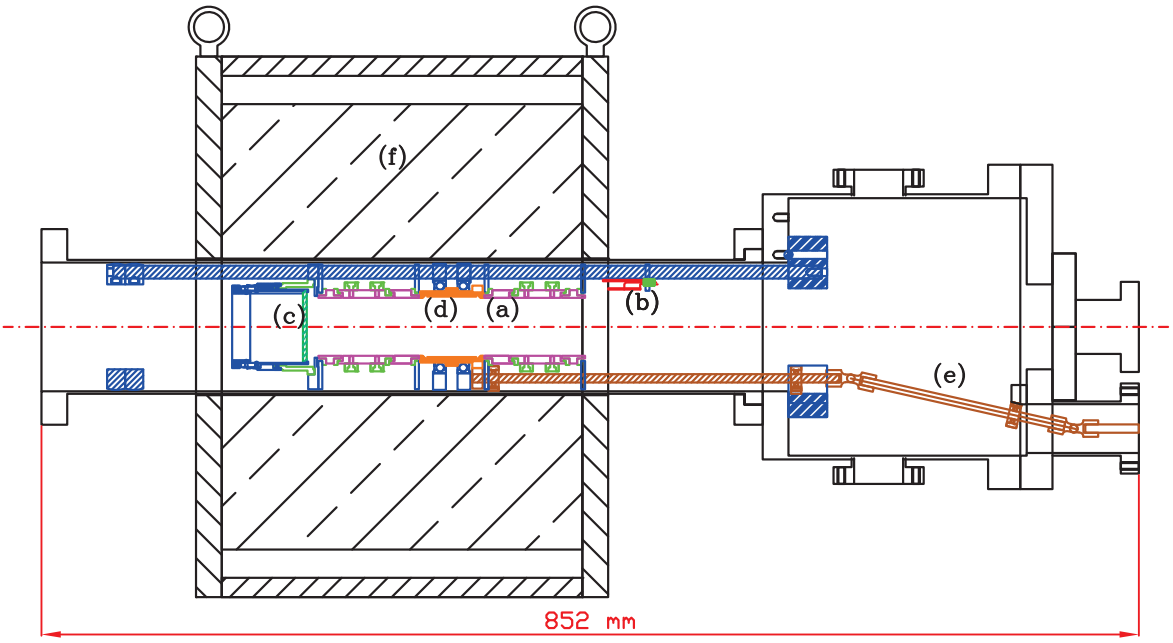

FIGURE 1. Sketch of the dusty-plasma compact trap: vertical section (except for the mounting bars, rotated by 45 degrees around the z-axis). A tower-like stack of electrodes (a), separated by insulating spacers, is inserted into the vacuum bore. At the two ends of the stack, off-axis thermocathodes (b) and a phosphor screen (c) are installed. The longer electrode in the middle (d) has a microstructured inner surface loaded with dust grains and can be set in rotation by means of a drive shaft (e), connected via a rotary motion vacuum feedthrough to an external electric motor. The off-axis placement of the shaft allows for axial optical access to the trapping region. The whole vacuum vessel is surrounded by a normal-conducting solenoid magnet (f), see Fig. 2.

for the electrons and a kinetic description for the dust component (including gravity). In order to investigate the influence of the dust on the development of the diocotron instability in the electron plasma, simulations with different initial dust distributions have been performed. In particular, the early stage of the growth of diocotron modes has been analyzed by means of a Fourier decomposition. A few examples of numerical results are reported here.

EXPERIMENTAL SET-UP

For the confinement of a dust-contaminated electron plasma, a dedicated apparatus is presently under construction at the Department of Physics of the University of Milano. The multipurpose linear magneto-static device DuEl, sketched in Fig. 1, is based on a Penning-Malmberg trap scheme [11, 12] with the possibility of feeding background gas and/or a (sub-)micrometric dust contaminant. A cylindrical vacuum vessel (inner diameter 100 mm), evacuated down to the UHV regime by a turbo-molecular pumping system, is surrounded by a normal-conducting solenoid producing an axial field up to 0.9 T (see Fig. 2). The device features a stack (approximate length 200 mm) of hollow cylindrical electrodes with an inner diameter of 45 mm, separated by polyether ether ketone (PEEK) spacers. Two of the electrodes are azimuthally segmented into four electrically insulated patches, held into their positions by means of PEEK rings (see Fig. 3). The electrodes and their azimuthal sectors can be individually biased to suitable electric potentials in order to create an electrostatic axial trapping well, to apply a RF excitation and in general to manipulate the axial and azimuthal dynamics of the plasma. The azimuthal sectoring of the electrodes also allows for the diagnostics of transverse-plane collective properties of the plasma, e.g. space-charge [13] and fluid instabilities [14]. A set of thermionic sources placed at one end of the stack will provide a continuous stream of electrons, which can be detected by the optical radiation produced by the beam impacting on a phosphor screen at the other end of the electrode structure. A number of phenomena related to the interaction of RF-heated electron samples with a background gas, e.g. ionization, collective oscillations and suppression of transverse instabilities, have been already investigated in a different apparatus [15, 16]. A gas inlet will be installed in the DuEl device in order to systematically study such

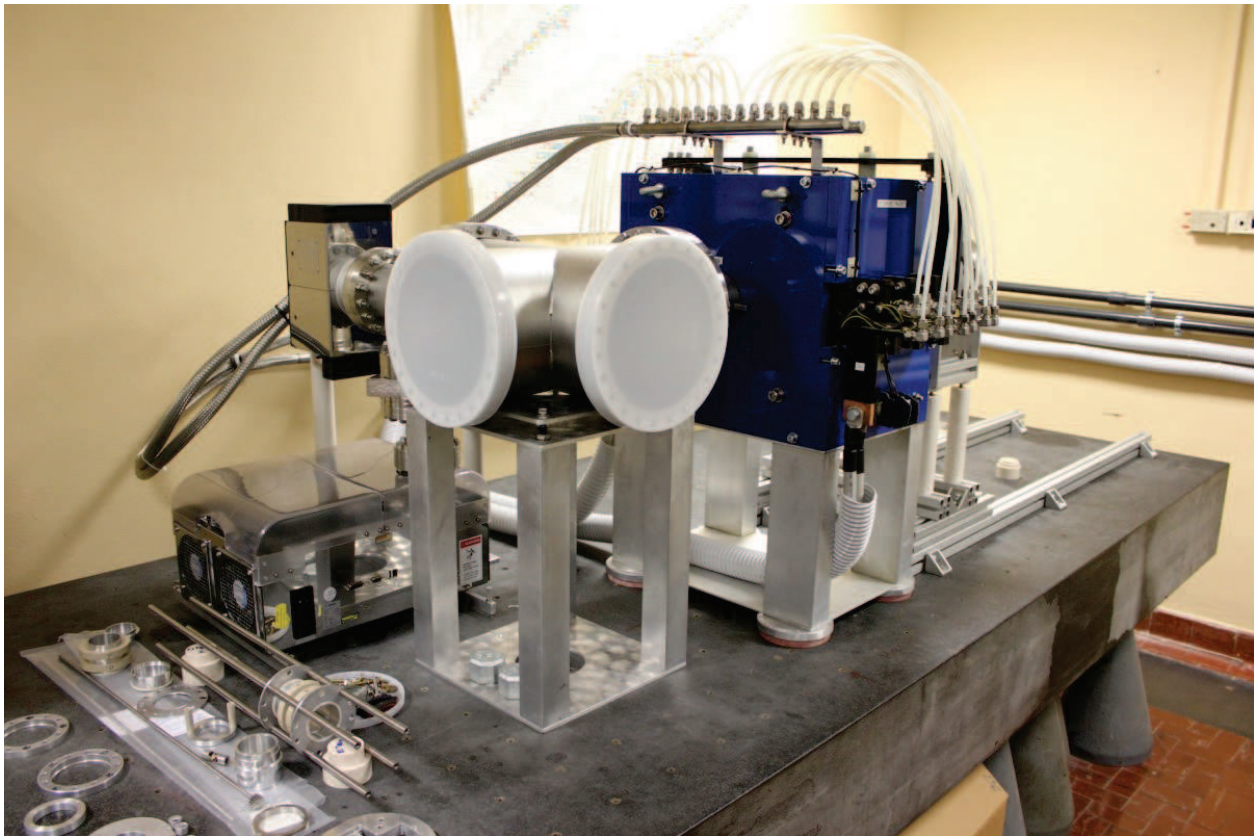

FIGURE 2. Picture of the DuEl apparatus in the assembly stage in the Plasma Physics Laboratory of the Department of Physics, University of Milano (Italy). The pumping system and the normal-conducting solenoid magnet can be seen in the front and in the back, respectively.

features.

The dust dispenser is a specially designed electrode which can be set in rotation via a drive shaft connected to an electric motor (see Fig. 1). The inner surface of this electrode is covered with a metallic 'carpet', which can be loaded with dust grains with a diameter from 50 nm to several micrometers [17]. The rotation will cause the dust grains to drop through the electron flow thus acquiring a negative charge. The phosphor screen will be removable to allow for an axial line of sight. An optical detection of the dust is envisaged by means of self-referenced interferometry of a laser light scattered by the dust grains [18].

PHYSICAL MODEL

We consider an electron plasma contaminated by a population of negatively charged dust particles contained in a cylindrical domain of radius R_w, and confined radially by a constant and uniform magnetic field, $\mathbf{B} = B\mathbf{e}_z$ directed along the axis of the trap. Under conditions of strong magnetization of the electron component, an electrostatic cold fluid description of the electron dynamics is adopted, in which electron inertia effects are neglected [4]. In this limit, the electron plasma dynamics becomes isomorphic to that of a 2D incompressible inviscid fluid, where the fluid vorticity corresponds to the electron density and the fluid stream function to the electrostatic potential [7]. On the contrary, the magnetization of the dust population is typically only marginal, since the charge-to-mass ratio of dust grains is several orders of magnitude smaller than that of the electrons and their Larmor radius may become larger than R_w. As a consequence, the dynamics of the massive particle population must be treated kinetically.

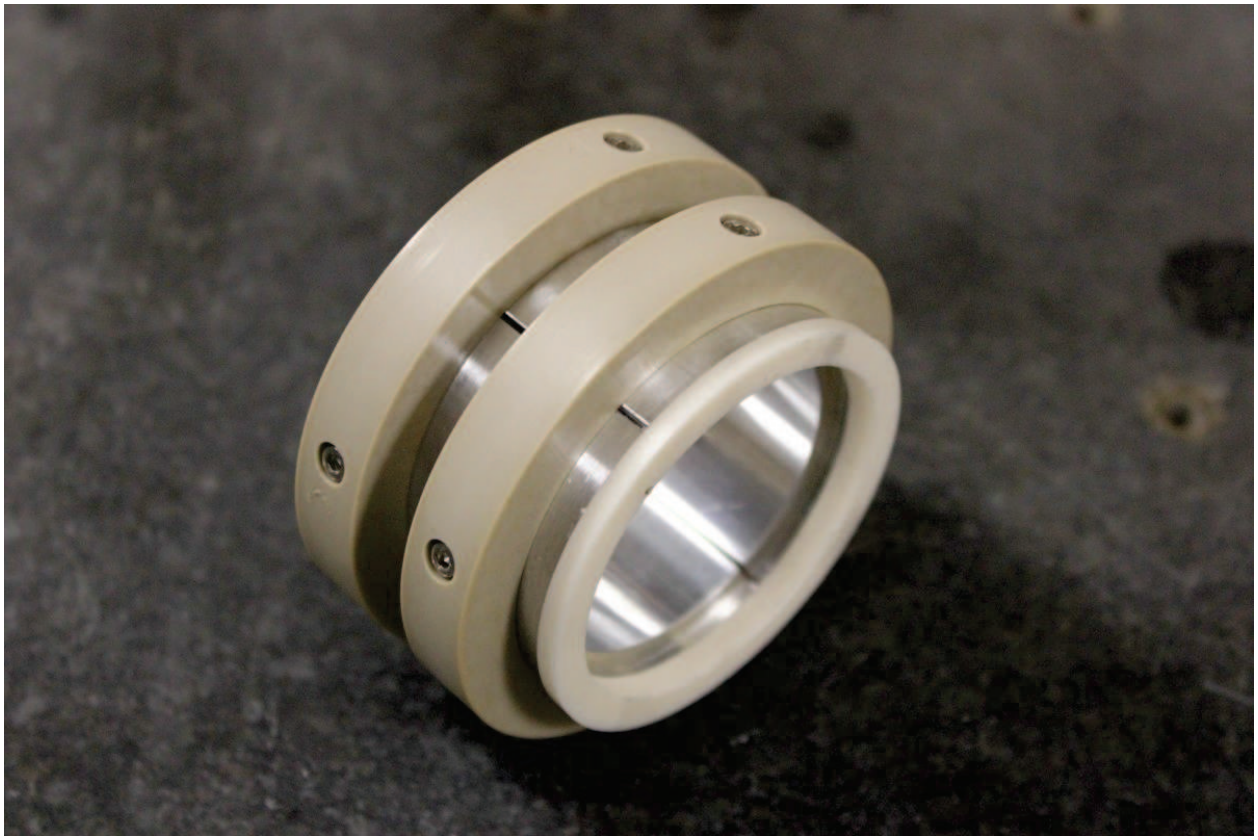

FIGURE 3. Picture of an azimuthally sectored electrode, built of four insulated parts, positioned 90 degrees from each other.

The equations governing the transverse dynamics of the multispecies system under consideration are therefore written as

$$\frac{\partial n_e}{\partial t} + [\phi, n_e] = 0, \tag{1}$$

$$\frac{\partial f_d}{\partial t} + \mathbf{v}\cdot\nabla f_d + \left[\frac{Z_d e}{m_d}(-\nabla\phi + \mathbf{v}\times\mathbf{B}) + \mathbf{g}\right]\cdot\frac{\partial f_d}{\partial \mathbf{v}} = 0, \tag{2}$$

$$\nabla^2\phi = \frac{e}{\varepsilon_0}\left(n_e - Z_d\int d^2v f_d\right). \tag{3}$$

Here, (r,θ) are polar coordinates in the transverse plane, n_e denotes the electron density, $f_d(r,\theta,v_r,v_\theta)$ is the distribution function of the massive particle population (integrated over the axial velocity v_z), ϕ is the electrostatic potential, $-e$ the electron charge, $Z_d < 0$ the charge number of the dust grains, m_d their mass, $\mathbf{g} = -g\mathbf{e}_y$ the gravity acceleration, and $d^2v = dv_r dv_\theta$ the surface element in the transverse velocity space. Finally, the bracket $[f,h]$ between two functions f and h of the spatial variables (r,θ) is defined as $[f,h] = (1/Br)(\partial_r f\partial_\theta h - \partial_\theta f\partial_r h)$.

Eq. (1) represents the continuity equation for the electron density, advected by the incompressible $\mathbf{E}\times\mathbf{B}$ flow. Eq. (2) is a Vlasov equation that governs the evolution of the massive particle population, whereas Eq. (3) is the Poisson's equation determining the electrostatic potential. The equations form a noncanonical Hamiltonian system [19], characterized by the existence of two independent families of Casimir invariants, given by $C_1 = \int dA\mathscr{F}(n_e)$ and $C_2 = \int dAd^2v\mathscr{G}(f_d)$, with $\mathscr{F}$ and $\mathscr{G}$ arbitrary functions. The invariants include, as particular cases, the familiar invariants of the 2D Euler incompressible equations [20, 9], such as the enstrophy, and those of the Vlasov equation, such as the entropy. In particular, the Hamiltonian structure of the model can be used to derive a set of stability conditions for rotating coherent structures of the two-species system. Stability is obtained if both the dust distribution function

and the density of the electron fluid at the equilibrium are monotonically decreasing functions of the corresponding single-particle energies in the rotating frame [19].

NUMERICAL INVESTIGATIONS

The numerical solution of the model equations (1)-(3) has been accomplished with the development of a new particle-in-cell (PIC) code [10]. In order to describe also quasi-neutral or partially neutralized plasmas, three particle species can be treated by the code, namely electrons, dust grains and positive ions.

Using a cartesian grid, the Poisson equation is solved by means of a 2D Fast Fourier Transform (FFT) combined with a capacity matrix method [21]. Static and/or time-dependent Dirichlet boundary conditions are imposed on a sequence of sides of grid cells, which represent a piecewise linear approximation of a circumference. This allows one to simulate, e.g., a resistive dissipation or radio-frequency excitations applied on the cylindrical trap electrodes, which may be sectored into multiple electrically separated azimuthal patches.

For the particle advancement, different algorithms are available in the code for each species. The guiding center approximation adopted for the electrons allows for simulation time steps by several orders of magnitude larger than the electron cyclotron period. The integration method is in this case a standard fourth-order Runge-Kutta scheme. On the other hand, the kinetic treatment for dust grains and ions is accomplished implementing a B-field modified Velocity Verlet algorithm [22, 23].

For simplicity dust grains are modelled as dielectric particles with a given surface charge, whose value may be estimated considering the grains as spherical capacitors (e.g., in a plasma with a space charge potential of a few volts, $Z_d \simeq -100$ on a dust grain with a 100 nm diameter). The modelling of an electron density-dependent floating charge on the dust grains is presently under development, as well as the implementation of Monte-Carlo schemes to model collisions of the particles with the buffer-gas.

The simulations presented here have been performed using a set of parameters similar to those of the future experiments with the DuEl apparatus [8] and suitable to describe the insurgence of the diocotron (Kelvin-Helmholtz) instability in the magnetized electron plasma and the influence of a dust contamination on its development. Zero potential is assumed on a circular boundary with radius $R_w = 20$ mm, inscribed in a square domain discretized by 257×257 nodes. The magnetic field is 1 T. Electron plasmas with uniform density $n_e = 10^7$ cm^{-3} over annular cross-sections are considered. The outer and inner ring radii have been chosen as $0.45R_w$ and $0.36R_w$, respectively. Dust grains are assigned a charge number $Z_d = -100$. The mass is computed considering spherical grains with a diameter of 100 nm and a density 1.05 g/cm^3 (typical of polymeric particles). The time step is 0.15 μs and the total simulation time is of a few milliseconds (sufficient to follow the complete evolution of the diocotron instability).

In a first set of simulations a contamination of the whole electron ring is considered. The electron fluid is modelled by $5 \cdot 10^5$ macroparticles, while the dust population is represented by $1 \cdot 10^5$ macroparticles with zero initial velocity. The dust fraction n_d/n_e ranges from $5 \cdot 10^{-4}$ to $3 \cdot 10^{-3}$. The electron density is correspondingly depleted, assuming that the dust grains acquire their charge from that of the electrons. In Fig. 4 time sequences of electron and dust distributions are shown (along the rows) for increasing dust contamination. The evolution of the pure electron annulus is dominated by the $m = 5$ diocotron mode, leading to the formation of five long-lived vortices, in agreement with theory [4]. When dust is added, the development of the diocotron instability is clearly modified. The dust component in these simulations is not effectively confined and expands radially. Although this situation can not reproduce real experimental conditions, it highlights the clear influence of dust contamination on the dynamics of the electron plasma. In particular, a damping of the higher order diocotron modes and a growth of the low-order modes occur, leading to vortex merger events. Increasing the dust contamination, the sequence of merger events of the electron vortices up to the collapse to a single clump becomes more rapid.

In a second set of simulations an asymmetric contamination was assumed in order to model initially neutral dust grains dropping down vertically through the plasma cross section (a situation envisaged in the DuEl apparatus). The electron annulus is the same as in the previous cases. The electron fluid is again modelled by $5 \cdot 10^5$ macroparticles, while $3.75 \cdot 10^4$ dust macroparticles are placed in the upper circular segment of the electron ring. The electron density and the number of electron macroparticles are correspondingly reduced in this region. Simulations have been performed for different dust contaminations (n_d/n_e ranging from $3 \cdot 10^{-4}$ to $3 \cdot 10^{-3}$) and for different initial fall velocities.

In Fig. 5 the first row shows the case of $n_d/n_e = 5 \cdot 10^{-4}$ in the contaminated upper circular segment with an initial dust velocity corresponding to the free fall from the top boundary, while in the second row the initial velocity is increased by a factor of 10. Using the same two values of the fall velocity, the results for the case of a higher dust

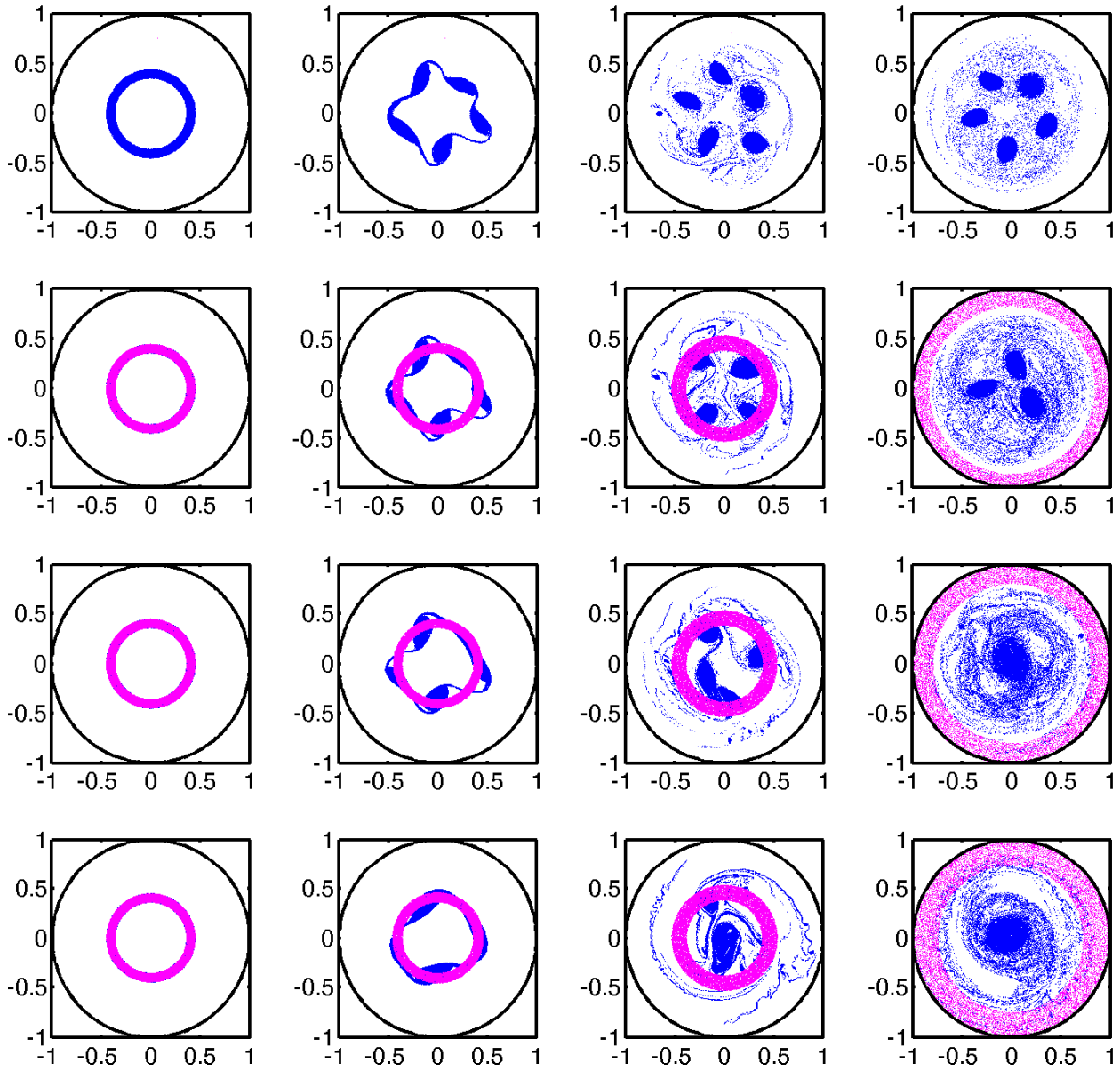

FIGURE 4. Evolution of an electron plasma with initial uniform annular density profile and increasing fraction of uniform dust contamination. First row: Pure electron plasma with $n_e = 10^7$ cm^{-3}. In the lower rows, electrons are contaminated by dust grains with $Z_d = -100$. Electron density is depleted accordingly. Second row: Dust density $n_d = 5 \cdot 10^3$ cm^{-3}. Third row: $n_d = 1.5 \cdot 10^4$ cm^{-3}. Fourth row: $n_d = 3 \cdot 10^4$ cm^{-3}. Blue and magenta dots correspond to electrons and dust particles, respectively. Only 5% of the simulation macroparticles are plotted. Spatial coordinates are normalized to a trap radius $R_w = 20$ mm. For all sequences the times are, from left to right, 0, 210 μs, 675 μs and 2.1 ms, and $B = 1$ T.

density, $n_d/n_e = 2 \cdot 10^{-3}$, are shown in the last two rows. As in the case of symmetric dust contamination, increasing the dust fraction the collapse of the electron fluid to a single clump turns out to be accelerated. For low values of the initial fall velocity, the dust is gradually expelled from the electron plasma and its effect is limited to the early stage of the evolution. Increasing the injection velocity the dust population remains for a longer time in the central region of the trap, and its prolonged influence leads to a faster evolution of the diocotron instability and to a more rapid collapse of the electron coherent structures.

A more quantitative determination of the influence of the dust is obtained from the Fourier analysis of the early stage of the growth of the diocotron instability [10]. The difference between the potential at a given time t and its

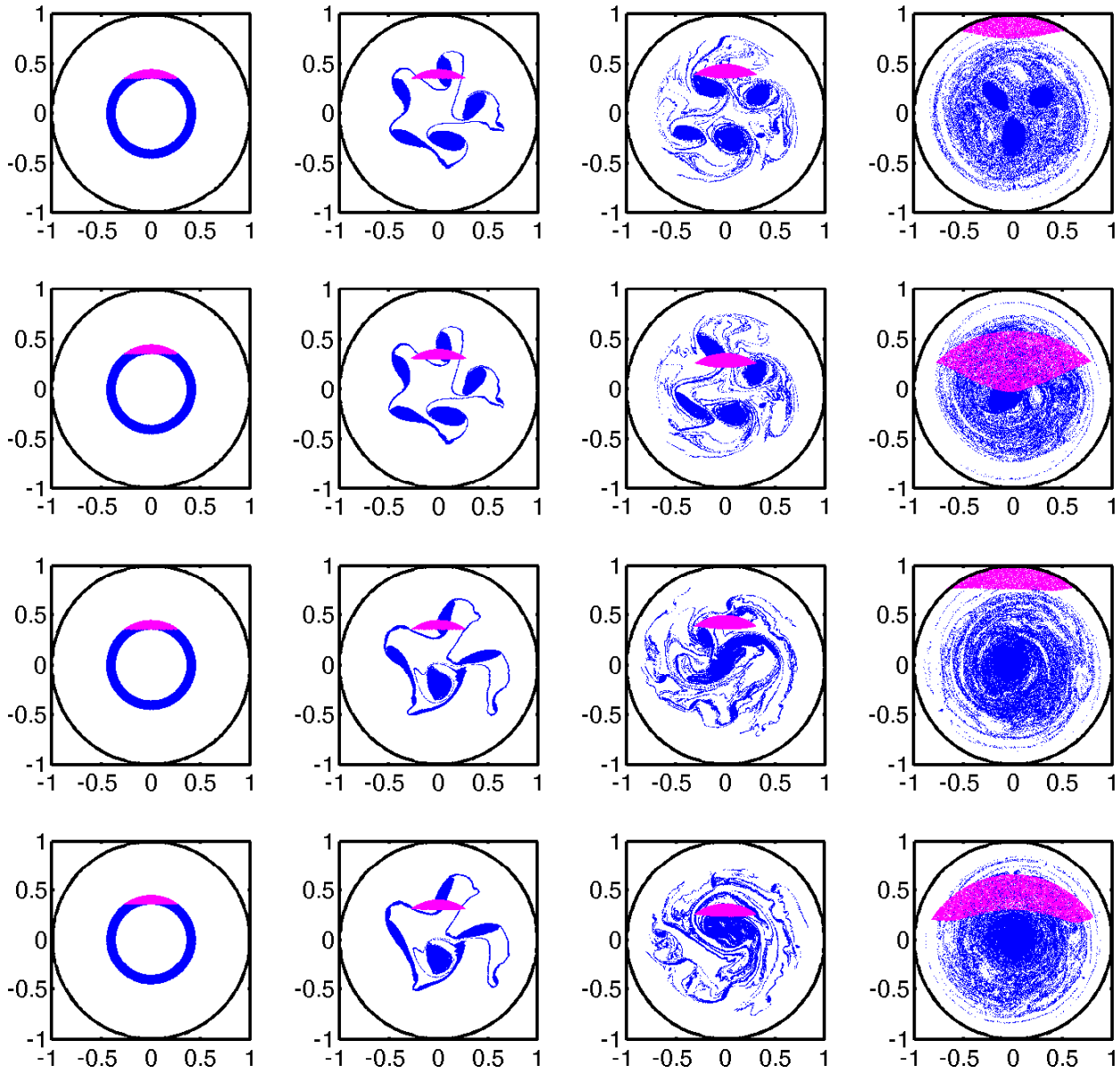

FIGURE 5. Evolution of electron plasma rings with the upper circular segment contaminated by dust ($Z_d = -100$) with varying densities and fall velocity. The unperturbed electron density is $n_e = 10^7$ cm^{-3}. First row: Dust density $n_d = 5 \cdot 10^3$ cm^{-3} and vertical velocity -0.45 m/s. Second row: As above, with vertical velocity -4.5 m/s. Third row: Dust density $n_d = 2 \cdot 10^4$ cm^{-3} and vertical velocity -0.45 m/s. Fourth row: As above, with vertical velocity -4.5 m/s. Blue and magenta dots correspond to electrons and dust particles, respectively. Only 5% of the simulation macroparticles are plotted. Spatial coordinates are normalized to a trap radius $R_w = 20$ mm. For all sequences the times are, from left to right, 0, 240 μs, 600 μs and 2.1 ms, and $B = 1$ T.

initial value is calculated starting from the particle distributions computed at the same time instant, and expanded in a truncated Fourier series in the azimuthal angle θ as

$$\delta\phi(r,\theta,t) = \sum_{m=-\infty}^{+\infty} \delta\phi^m(r,t)\exp(im\theta). \tag{4}$$

The power of the m-th mode is then computed as

$$A_m(t) = 2\pi \int_0^{R_w} |\delta\phi^m(r,t)|^2 \, r dr, \tag{5}$$

and fitted to an exponential function to obtain the growth rate $2\gamma_m$. For the annular configuration considered in the simulations reported here, the analysis for the pure electron plasma case indicates that modes 2 to 6 are unstable, with maximum growth rate for the $m = 5$ mode [4]. This is in qualitative agreement with the time evolution of the system observed in the first row of Fig. 4. The initial perturbation of the flat annular profile is given by the slight asymmetries of the numerically assigned initial particle distributions, and by the discretization of the annulus on the cartesian grid.

For the first set of simulations, i.e. with a uniform dust contamination, the growth rates γ_m for $m > 4$ turn out to become smaller for increasing dust density at the expense of growing low-order modes ($m = 1 - 3$). Eventually this leads to more rapid vortex merger events as previously noticed. The analysis of the second set of simulations, i.e. dust contamination in the upper circular segment only, similarly shows that the originally dominant $m = 5$ mode is increasingly damped for increasing dust fractions. As a consequence of the asymmetry of the initial configuration, lower-order modes are always present. The $m = 1$ is particularly intense, and becomes dominant for $n_d/n_e \geq 10^{-3}$, as evidenced from the rapid formation of a large central clump in the two lower sequences of Fig. 5.

To summarize, several PIC simulations have been performed in order to characterize the effects of dust on the formation and evolution of coherent structures in the electron plasma. Depending on the dust fraction and its initial distribution, a partial damping of the diocotron instability at higher mode numbers has been observed, although with asymmetric dust contaminations the number of active modes becomes larger. Further investigations using different sets of dust parameters (size, charge, injection velocity) are planned. In addition, the PIC code will be upgraded in order to investigate other phenomena of interest, e.g. dust charging or collisions with neutrals.

ACKNOWLEDGMENTS

The DuEl Project has been supported by INFN National Scientific Committee V (technological researches) and by the Italian Ministry for University and Research (MIUR) “PRIN 2009” funds (Grant No. 20092YP7EY).

REFERENCES

1. G. E. Morfill and A. V. Ivlev, *Rev. Mod. Phys.* **81**, 1353 (2009).
2. E. Thomas Jr., R. L. Merlino and M. Rosenberg, *Plasma Phys. Control. Fusion* **54**, (2012) 124034.
3. E. Thomas Jr., A. M. DuBois, B. Lynch, S. Adams, R. Fisher, D. Artis, S. LeBlanc, U. Konopka, R. L. Merlino, and M. Rosenberg, *J. Plasma Phys.* **80**, 803 (2014).
4. R. C. Davidson, *Physics of Nonneutral Plasmas*, Addison-Wesley, Redwood City, 1990.
5. T. M. O’Neil, *Phys. Today* **52**, 24 (1999).
6. G. B. Andresen and the ALPHA Collaboration, *Nature Phys.* **7**, 564 (2011).
7. C. F. Driscoll and K. S. Fine, *Phys. Fluids B* **2**, 1359 (1990).
8. M. Maggiore, M. Cavenago, M. Comunian, F. Chirulotto, A. Galatà, M. De Lazzari, A. M. Porcellato, C. Roncolato, S. Stark, A. Caruso, A. Longhitano, F. Cavaliere, G. Maero, B. Paroli, R. Pozzoli, and M. Romé, *Rev. Sci. Instrum.* **85**, 02B909 (2014).
9. M. Romé and F. Lepreti, *Eur. Phys. J. Plus* **126**, 38 (2011).
10. G. Maero, M. Romé, F. Lepreti, and M. Cavenago, *Eur. Phys. J. D* **68**, 277 (2014).
11. D. Dubin and T. M. O’Neil, *Rev. Mod. Phys.* **71**, 87 (1999).
12. M. Amoretti, G. Bettega, F. Cavaliere, M. Cavenago, F. De Luca, R. Pozzoli, and M. Romé, *Rev. Sci. Instrum.* **74**, 3991 (2003).
13. B. Paroli, G. Bettega, F. Cavaliere, F. De Luca, G. Maero, R. Pozzoli, M. Romé, M. Cavenago, and C. Svelto, *J. Phys. D: Appl. Phys.* **42**, 175203 (2009).
14. F. Lepreti, M. Romé, G. Maero, B. Paroli, R. Pozzoli and V. Carbone, *Phys. Rev. E* **87**, 063110 (2013).
15. B. Paroli, F. De Luca, G. Maero, R. Pozzoli, and M. Romé, *Plasma Sources Sci. Technol.* **19**, 045013 (2010).
16. B. Paroli, G. Maero, R. Pozzoli, and M. Romé, *Phys. Plasmas* **21**, 122102 (2014).
17. W. Xu, B. Song, R. L. Merlino, and N. D’Angelo, *Rev. Sci. Instrum.* **63**, 5266 (1992).
18. F. Ferri, D. Magatti, D. Pescini, M. A. C. Potenza, and M. Giglio, *Phys. Rev. E* **70**, 041405 (2004).
19. E. Tassi, M. Romé, and C. Chandre, *Phys. Plasmas* **21**, 044504 (2014).
20. M. Romé, M. Brunetti, F. Califano, F. Pegoraro, and R. Pozzoli, *Phys. Plasmas* **7**, (2000) 2856.
21. R. W. Hockney and J. W. Eastwood, *Computer Simulation Using Particles*, McGraw-Hill, New York, 1981.
22. Q. Spreiter and M. Walter, *J. Comput. Phys.* **152**, 102 (1999).
23. G. Maero, F. Herfurth, H.-J. Kluge, S. Schwarz, and G. Zwicknagel, *Appl. Phys. B* **107**, 1087 (2012).